Viscoelastic Behavior and Fragility of Se-deficient Chalcogenide Liquids in As-P-Se System

[1]Bing Yuan, [2]Bruce G. Aitken, [1]Sabyasachi Sen*

[1]Department of Materials Science & Engineering, University of California at Davis,

Davis, CA 95616, USA

[2]Science & Technology Division, Corning Inc., Corning, NY 14831, USA

*Corresponding Author: Sabyasachi Sen (email: sbsen@ucdavis.edu)

ABSTRACT

The viscoelastic behavior of supercooled Se-deficient liquids in the series As_xSe_{100-x} ($40 \leq x \leq 60$) and $P_xAs_{4-x}Se_3$ ($0 \leq x \leq 2.8$) are studied using parallel plate rheometry. The compositional variations in the viscosity and fragility of these liquids are shown to be consistent with the corresponding structural evolution. While the shear relaxation of As_xSe_{100-x} liquids with $40 \leq x \leq 50$ is associated with the dynamics of As-Se bond scission/renewal, the As-rich liquids with $x \geq 55$ are found to display an additional low-frequency process, which is related to a cooperative interconversion between molecular and network structural moieties. A similar behavior is also exhibited by the As-rich liquids in the $P_xAs_{4-x}Se_3$ series. In contrast, the P-rich liquids characterized by high molecule content display a power-law relaxation behavior resulting from a rather broad distribution of relaxation timescales associated with various dynamical modes of single molecules and molecular clusters.

1. INTRODUCTION

Chalcogenide glasses that are primarily sulfides, selenides or tellurides of group IV and/or V elements, namely Ge, Si, As, P and Sb have found important technological applications in areas ranging from photonics and environmental remote sensing to energy and memory storage [1–7]. The remarkable compositional flexibility of chalcogenides allows for excellent tuning of their electronic and optical properties. On the other hand, their atomic structure is intimately linked to the viscoelastic behavior of the parent liquids, and therefore a mechanistic understanding of this link is essential for their compositional optimization for various processing techniques [8,9].

Binary Ge-Se and As-Se glasses have long served as the model systems for understanding the role of structure on the physical properties of chalcogenide glasses and liquids. The structural control on the viscoelastic behavior of supercooled Se-rich Ge-Se and As-Se glass-forming liquids has been studied extensively in the past using small amplitude oscillatory shear (SAOS) rheometry [10–13]. These studies have demonstrated that in pure Se the primary structural building blocks are polymeric $[Se]_n$ chains formed by two coordinated Se atoms and the corresponding rheological behavior is shown to be characterized by two coexisting dynamical processes, the fast segmental chain motion, and the slow Se-Se bond scission/renewal process. In the case of the As-Se system the progressive addition of As atoms up to ~15 at.% As results in the formation of pyramidal $AsSe_{3/2}$ units, which cross-link the $[Se]_n$ chains and the average chain length decreases [14,15]. This structural evolution results in a progressive decrease in the difference between the fast and slow dynamical processes in their timescale and eventually the fast relaxation process vanishes when the average length of the $[Se]_n$ chains becomes shorter than ~ 3 to 5 Se atoms [10]. Further increase in the As content results in a rigid three-dimensional network consisting predominantly of corner-shared $AsSe_{3/2}$ pyramids with only minor violation in the chemical order [14,15]. At this point, the rheological behavior of the $As_{30}Se_{70}$ liquid was shown to be consistent with the structural relaxation being entirely controlled by the As-Se bond scission/renewal process [16].

Previous structural studies have indicated that in contrast to Se-rich and stoichiometric compositions, the structure of Se-deficient compositions with As >40 at.% consists of As-As homopolar bonds [14,15]. As expected, the relative concentration of these homopolar bonds increases progressively with increasing As content and results in the formation of cage like As_4Se_3 molecules and tetrahedral As_4 molecules and/or fragments of two-dimensional sheets of corner-shared As_4 tetrahedra. However, unlike the Se-rich and stoichiometric As-Se liquids, the role of homopolar bonding and of the various associated low-dimensional structural moieties in controlling the rheological behavior of Se-deficient liquids has never been investigated in the past, in a systematic fashion. It may be noted here that besides the frequency-dependent viscoelastic relaxation behavior, even the true nature of the compositional variation of viscosity remains somewhat unclear in these As-rich As-Se glass-forming liquids. Previous studies of viscosity measurements by Nemilov et al. and Kunugi et al., which are the only such studies in the literature to the best of our knowledge, yielded inconsistent datasets on stoichiometric and Se-deficient (Se $\leqslant$ 60 at.%) As-Se compositions [17,18]. The viscosity datasets on identical compositions reported in these two studies often differ by more than 0.5 order of magnitude. Moreover, while Kunugi et al.'s viscosity data are characterized by relatively large error bars, those reported by Nemilov et al. are characterized by rather abrupt changes in the temperature dependence of viscosity over different temperature ranges, which appear to be somewhat unphysical [17,18]. Therefore, in order to address this gap in knowledge, a systematic investigation of the rheological behavior of Se-deficient As-Se liquids is carried out in the present work.

A recent rheological study of predominantly molecular P-rich P-Se liquids that contain cage like P_4Se_3 molecules has indicated that such liquids are characterized by a rather unique power-law viscoelastic relaxation behavior [19]. Like gels, the dynamic viscosity of these molecule-rich liquids shows a departure from the Maxwell-type behavior in the frequency dependence of the storage and loss shear moduli. Such behavior is accompanied by a clear enhancement of the dynamic viscosity over that of network liquids at frequencies below the onset of the dynamical behavior with the apparent lack of a frequency-independent regime. It is therefore interesting to extend such studies to investigate whether this "anomalous" behavior is universal and can be observed in other molecule-rich chalcogenides. Although, as noted above, cage like As_4Se_3 molecules that are geometrically similar to the P_4Se_3 molecules appear in the structure of Se-deficient As-Se glasses, their relative fraction is significantly lower than that observed in the P-Se glasses with compositions close to the P:Se = 4:3 ratio. Keeping this fact in mind we extend the rheological study of such molecular liquids along the As_4Se_3–P_4Se_3 pseudobinary join. Accordingly, here we report a comprehensive study of the rheological behavior of Se-deficient As_xSe_{100-x} ($40 \leq x \leq 60$) and $P_xAs_{4-x}Se_3$ ($0.4 \leq x \leq 2.8$) chalcogenide liquids using parallel plate rheometry to investigate the structural control on their viscoelastic behavior. The structure of the $P_xAs_{4-x}Se_3$ glasses is characterized using Raman spectroscopy. The corresponding compositional variations in the temperature dependence of their viscosity are discussed.

2. EXPERIMENTAL

2.1 Sample Synthesis and Physical Characterization

The As_xSe_{100-x} glasses ($40 \leq x \leq 60$) and $P_xAs_{4-x}Se_3$ glasses ($0 \leq x \leq 2.8$) were prepared in ~12g batches from the constituent elements (⩾99.999% purity, metal basis) by the conventional melt-quench method. The mixtures of constituent elements were loaded into quartz ampoules that were fused and evacuated to 10^{-4} Torr. The ampoules were then loaded in a rocking furnace, slowly heated to 600 ºC over 13 hours and held at this temperature for 36 h to ensure melt homogeneity. The melts were subsequently quenched to form glasses by dipping the ampoules in water. All $P_xAs_{4-x}Se_3$ glasses were cooled and held at 350 ºC for an additional 2 h prior to quenching. The Raman spectra of all $P_xAs_{4-x}Se_3$ glasses were collected in a backscattering geometry with a resolution of 1 cm^{-1} using a Renishaw 1000 Raman spectrometer equipped with a microscope and a He-Ne laser operating at a wavelength of 633 nm. The backscattered light was detected using a charge-coupled device cooled to 200K.

2.2. Parallel Plate Rheometry

All rheological measurements were carried out on an Anton-Paar MCR 302 parallel plate rheometer equipped with a convection oven (up to 600 ºC) under constant nitrogen gas flow. All samples were first heated inside the oven above their softening point, then trimmed into a disc geometry with ~ 1 mm thickness, which was sandwiched between the 8 mm oscillating upper plate and the stationary lower plate. At each temperature the sample was allowed to equilibrate for 5 min for all measurements. For SAOS measurements an oscillatory strain within the linear viscoelastic region was applied with varying angular frequency ω between 1 to 600 rad/s and the induced torque was recorded to calculate the storage and loss moduli G' and G'' as a function of ω. Measurements were carried out at multiple temperatures for each sample and master curves of $G'(\omega)$ and $G''(\omega)$ were constructed using time-temperature superposition (TTS). The Newtonian viscosity η was determined under steady shear as the ratio of stress to strain rate $\dot{\gamma}$ at various strain rates ranging between 0.01 s^{-1} and 1 s^{-1} at each temperature.

3. RESULTS AND DISCUSSION

3.1. Rheological behavior of As_xSe_{100-x} liquids

The experimental G′(ω) and G″(ω) master curves for these As_xSe_{100-x} supercooled liquids in the composition range $40 \leq x \leq 60$, constructed at iso-viscous temperatures corresponding to ~ 10^8 Pa.s are shown in Fig. 1. At low frequencies, in the terminal regime, all liquids exhibit G′ < G″ and follow the frequency scaling of $G' \sim \omega^2$ and $G'' \sim \omega$, as expected from the Maxwell model. On the other hand, in the high frequency elastic regime the G′(ω) reaches a plateau that is on the order of a few GPa and this plateau represents the high-frequency glassy shear modulus G_∞. The $As_{40}Se_{60}$, $As_{45}Se_{55}$ and $As_{50}Se_{50}$ liquids display a simple viscoelastic behavior with a single dynamical process with an average relaxation timescale denoted by the G′ - G″ crossover. Previous studies have shown that this dynamical process is associated with local As-Se bond scission/renewal in the liquid [12,16]. Further increase in the As content results in a clear change in the frequency scaling of G′ from ~ ω^2 in the terminal regime to ~ ω^a, with $a \sim 1.3$, in the intermediate frequency regime over nearly 3 orders of magnitude variation in frequency before the G′ - G″ crossover (Fig. 1). Such change in G′ slope indicates the emergence of a new dynamical mode and consequently the $As_{55}Se_{45}$, $As_{57.1}Se_{42.9}$ and $As_{60}Se_{40}$ liquids are characterized by two relaxation processes. Indeed, the G′(ω) and G″(ω) master curves of these liquids can be simulated well with two distinct relaxation processes that are characterized by significantly different timescales and G_∞ values (Fig. 2). While the fast (high-frequency) dynamics, characterized by a G_∞ of a few GPa, can be readily assigned to the local bond scission/renewal process observed in As_xSe_{100-x} supercooled liquids with $40 \leq x \leq 50$, the slow (low-frequency) dynamics may be indicative of the existence of a cooperative process involving a large group of atoms and with a much lower G_∞ on the order of ~ 1 MPa (Fig. 2). Structural studies of As_xSe_{100-x} glasses have shown that glasses with $x \geq 55$ are characterized by a relatively high concentration of tetrahedral As_4 and cage-like As_4Se_3 molecules [15]. A previous study reported the existence of a facile interconversion between As_4 molecules and polymeric chains of As atoms owing to a relatively low activation energy of polymerization [20]. A molecule-to-network interconversion could also be likely for the As_4Se_3 molecules [21]. Therefore, we hypothesize that the slow dynamical mode observed in the most Se-deficient As_xSe_{100-x} liquids with $x \geq 55$ is likely associated with such cooperative interconversion processes between molecular and network structural moieties.

The weak van der Waals interaction between these molecular units, present in significant concentration in As_xSe_{100-x} glasses with $x \geq 55$, and the consequent loss in connectivity are consistent with the compositional variation of the viscosity η of these liquids as shown in Fig 3. The isothermal viscosity decreases and the activation energy for viscous flow near glass transition increases monotonically with increasing As concentration in these supercooled liquids. Moreover, these parameters change rather sharply as x increases from 55 to 60 and the concentration of the molecular units is maximized. It is important to note that, compared to the previous reports in the literature, the viscosity data obtained in the present study exhibits a systematic compositional trend for the first time. The activation energy for viscous flow of a supercooled liquid near glass transition is often parametrized by the fragility index m, where $m = \left.\frac{d\log_{10}\eta}{dT_g/T}\right|_{T=T_g}$, and T_g is the glass transition temperature. The fragility index m for these As_xSe_{100-x} liquids is obtained by fitting the viscosity curves with the MYEGA equation [22,23]:

$$log\,\eta = log_{10}\eta_\infty + \frac{K}{T} \cdot exp\,(\frac{C}{T})$$

where $log_{10}\eta_\infty$, K, and C are all treated as fitting parameters. The fragility index m is subsequently calculated from these fitting parameters using the relation [23]:

$$m = \left(\frac{K}{T_g}\right)\left(1 + \frac{C}{T_g}\right)\exp\left(\frac{C}{T_g}\right)$$

The compositional variation of m obtained for these Se-deficient liquids are compared in Fig. 4 with those reported in the literature for the Se-excess liquids [24]. The general trend in m is quite similar to that reported in a previous study [25] where m of As_xSe_{100-x} liquids was determined using the calorimetric technique. The m value sharply decreases from pure Se to ~ 20 at.% As and reaches a plateau, which continues until the As content reaches ~ 40%. Beyond this point m increases rapidly as the As content increases to up to 60%. Previous theoretical models related the drop in m upon the initial addition of As to Se to the increasing degrees of crosslinking of the selenium chains, while the rise in m in the Se-deficient region has been ascribed to the formation of molecular units, which weaken the network connectivity thus, lead to an increase in m [25–27].

3.2. Structure and Rheological behavior of $P_xAs_{4-x}Se_3$ glasses and liquids

Unlike As_xSe_{100-x} glasses, the structure of $P_xAs_{4-x}Se_3$ glasses along the join has never been reported in the literature to the best of our knowledge. Here we present a structural analysis of these glasses based on their Raman spectra (Fig. 5). The structure of P-rich (> 55 at. %) P-Se glasses are known to primarily consist of cage-like P_4Se_3 molecules that are isostructural with the As_4Se_3 molecules [28–32], which appear in As-rich (> 55 at.% As) As-Se glasses, albeit at a significantly lower concentration. Although, unlike As_4Se_3, the P_4Se_3 liquid cannot be quenched to a glass at normal cooling rates, molecule rich glasses can be obtained for compositions with ~ 60% P content. The Raman spectrum of such a glass of composition $P_{63}Se_{37}$ is shown for comparison in Fig. 5, which shows relatively sharp bands located at ~133, 213, 366, and 484 cm^{-}

^{1}, all of which correspond to the various intramolecular modes of P_4Se_3 molecules. On the other hand, the Raman spectrum of As_4Se_3 glass is characterized by a broad band at ~224 cm^{-1} corresponding to the symmetric stretching of As-Se bonds in the pyramidal $AsSe_{3/2}$ units, and superimposed on it are two relatively sharp bands near ~ 203 and 236 cm^{-1} that correspond, respectively, to As_4 and As_4Se_3 molecular units with As-As homopolar bonds [15]. It may be noted that the 203 cm^{-1} band may also correspond to As clusters which consist of randomly corrugated two-dimensional sheets of 3-fold-coordinated As atoms [14]. The initial substitution of As with P in As_4Se_3 glass causes a drastic decrease in intensity of these molecular bands. The 203 cm^{-1} band disappears in the $P_{1.2}As_{2.8}Se_3$ glass and the 236 cm^{-1} band weakens drastically with further addition of P as the P:As atomic ratio reaches 1:1 in the $P_2As_2Se_3$ glass. As the P:As ratio continues to increase, new bands appear near 213 cm^{-1} and in the 300-500 cm^{-1} region in the Raman spectra of $P_{2.4}As_{1.6}Se_3$ and $P_{2.8}As_{1.2}Se_3$ glasses with the highest P:As ratios, that correspond to various P containing structural units including P_4Se_3 and possibly mixed $P_xAs_{4-x}Se_3$ molecules [33].

When taken together, these results suggest that the P atoms are first incorporated into the As-rich regions in the As_4Se_3 glass and converts the As_4 molecular units into network structures containing As-P heteropolar bonds. Further increase in the P content leads to the decrease in the relative concentration of As_4Se_3 molecules as indicated clearly by the decreasing intensity of the sharp band at ~236 cm^{-1}. The molecule:network ratio appears to reach a minimum for glasses with compositions $P_{1.6}As_{2.4}Se_3$ and $P_2As_2Se_3$. Beyond this point the molecule:network ratio in the structure increases again as mixed $P_xAs_{4-x}Se_3$ molecules form in significant concentration as is evidenced in the increase in intensity of a new band at ~345 cm^{-1} (Fig. 5). At the same time the P_4Se_3 molecules start to increase in concentration as evidenced by the growing intensity of the ~

366 cm^{-1} band (Fig. 5). A more quantitative estimate of the evolution of the molecule:network ratio in these glasses can be obtained by tracking the ratio of the intensities of the molecular bands at 203, 236 and 366 cm^{-1} corresponding, respectively, to As_4, As_4Se_3, and P_4Se_3 molecules, and the network band at 224 cm^{-1}. As can be seen in Fig. 6, this ratio indeed goes through a minimum for $P_xAs_{4-x}Se_3$ glasses with x in the range between 1.6 and 2.0. This compositional evolution of structure is consistent with the temperature dependence of the viscosity of $P_xAs_{4-x}Se_3$ liquids as shown in Fig. 7. It is clear that the isothermal viscosity monotonically increases with increasing P content as the molecule:network ratio decreases up to $P_2As_2Se_3$. Further increase in P content results in a decrease in isothermal viscosity, which is indicative of a decreasing structural connectivity as is indeed evidenced in the Raman spectra in the form of an increasing molecule:network ratio in the structure.

Finally, the corresponding viscoelastic behavior in the form of G′(ω) and G″(ω) master curves for these $P_xAs_{4-x}Se_3$ liquids are shown in Fig. 8. The two relaxation processes that were observed in As_xSe_{100-x} liquids with $x \geq 55$ clearly persist on replacing As with P in the $P_xAs_{4-x}Se_3$ liquids with at least up to $x = 0.8$. As noted above, beyond this point the molecule:network ratio rapidly decreases in these liquids and reaches a minimum in compositions $P_{1.6}As_{2.4}Se_3$ and $P_2As_2Se_3$. Consequently, the contribution of the molecule-to-network interconversion dynamics towards shear relaxation is expected to become increasingly weak. This expectation is borne out in the shear mechanical spectra of liquids with $1.2 \leq x \leq 2.0$ where the frequency dependence of the G′(ω) below the G′ - G″ crossover (Fig. 8) follows the Maxwell behavior and suggests the dominance of a single dynamical process associated with the network bond scission/renewal. As evidenced in the Raman spectra in Fig. 5, further increase in the P content results in a rapid increase in the molecule content in the liquids with P:As > 1:1, which is manifested in a departure from the

Maxwell behavior as both G′(ω) and G″(ω) scale nearly linearly with ω over the entire accessible frequency range below the G′-G" crossover and the terminal region displays a nearly constant ratio of G″/G′. As discussed above, such a viscoelastic relaxation behavior was recently observed in predominantly molecular binary P-Se liquids, which was ascribed to an extremely broad distribution of relaxation timescales resulting from the coexistence of various elementary and cooperative dynamical modes of single molecules and transient molecular clusters [19].

4. CONCLUSIONS

The shear mechanical response of supercooled As_xSe_{100-x} liquids in the composition range $40 \leq x \leq 60$ as evidenced in the frequency dependence of G′(ω) and G″(ω) indicates that the shear relaxation of As_xSe_{100-x} liquids with $40 \leq x \leq 50$ is associated with a single dynamical process that can be ascribed to the scission/renewal of As-Se bonds in the network. Increasing As content results in the formation and increasing concentration of As_4Se_3 and As_4 molecules in these liquids, and consequently a loss in structural connectivity. This structural evolution is manifested in a rapid lowering of isothermal viscosity and a sharp rise in m along with the appearance of an additional low-frequency dynamical process, which is related to a cooperative molecule-to-network interconversion. As-rich $P_xAs_{4-x}Se_3$ liquids along the pseudo-binary As_4Se_3-P_4Se_3 join share this dynamical behavior up to $x = 0.8$. Increasing replacement of As with P in this series results in a minimization of the molecule : network ratio for $1.2 \leq x \leq 2.0$ and the shear mechanical spectra of these liquids indicate that the slow molecule-to-network interconversion process ceases to be a major contributor to the shear relaxation. Further increase in the P content results in a rapid increase in the molecule content in the $P_xAs_{4-x}Se_3$ liquids with $x \geq 2.4$. The concomitant emergence of various dynamical modes of single molecules and transient molecular clusters results in an extremely broad distribution of relaxation timescales that is expressed in the shear mechanical spectra in the form of a power-law relaxation behavior.

ACKNOWLEDGEMENTS

This study is supported by the National Science Foundation Grant NSF-DMR 1855176. Jason A. Brown at Corning Inc. is thanked for his assistance with glass synthesis.

REFERENCES

[1] L. Calvez, Chalcogenide glasses and glass-ceramics: Transparent materials in the infrared for dual applications, Comptes Rendus Phys. 18 (2017) 314–322.

[2] J.M. Harbold, F.Ö. Ilday, F.W. Wise, J.S. Sanghera, V.Q. Nguyen, L.B. Shaw, I.D. Aggarwal, Highly nonlinear As–S–Se glasses for all-optical switching, Opt. Lett. 27 (2002) 119.

[3] C. Quémard, F. Smektala, V. Couderc, A. Barthélémy, J. Lucas, Chalcogenide glasses with high non linear optical properties for telecommunications, J. Phys. Chem. Solids. 62 (2001) 1435–1440.

[4] B. Bureau, X.H. Zhang, F. Smektala, J.L. Adam, J. Troles, H.L. Ma, C. Boussard-Plèdel, J. Lucas, P. Lucas, D. Le Coq, M. R. Riley, J. H. Simmons, Recent advances in chalcogenide glasses, J. Non. Cryst. Solids. 345&346 (2004) 276–283.

[5] A. Zakery, S.R. Elliott, Optical properties and applications of chalcogenide glasses: a review, J. Non. Cryst. Solids. 330 (2003) 1–12.

[6] P.A. Vermeulen, J. Momand, B.J. Kooi, Reversible amorphous-crystalline phase changes in a wide range of $Se_{1-x}Te_x$ alloys studied using ultrafast differential scanning calorimetry, J. Chem. Phys. 141 (2014) 024502.

[7] M. Wuttig, N. Yamada, Phase-change materials for rewriteable data storage, Nat. Mater. 6 (2007) 824.

[8] B.G. Aitken, S.C. Currie, B.C. Monahan, L.-M. Wu, E.W. Coonan, Chalcogenide glass for low viscosity extrusion and injection molding, US 7116888 B1, 2006.

[9] Q. Zheng, J.C. Mauro, Viscosity of glass-forming systems, J. Am. Ceram. Soc. 100 (2017) 6–25.

[10] S. Sen, Y. Xia, W. Zhu, M. Lockhart, B. Aitken, Nature of the floppy-to-rigid transition in chalcogenide glass-forming liquids, J. Chem. Phys. 150 (2019) 144509.

[11] W. Zhu, B.G. Aitken, S. Sen, Communication: Observation of ultra-slow relaxation in supercooled selenium and related glass-forming liquids, J. Chem. Phys. 148 (2018) 111101.

[12] W. Zhu, B. Aitken, S. Sen, Investigation of the shear relaxation behavior of As-Se liquids within the framework of entropic and elastic models of viscous flow, J. Non. Cryst. Solids. 534 (2020) 119959.

[13] W. Zhu, B.G. Aitken, S. Sen, Observation of a dynamical crossover in the shear relaxation processes in supercooled selenium near the glass transition, J. Chem. Phys. 150 (2019) 094502.

[14] D.C. Kaseman, I. Hung, Z. Gan, B. Aitken, S. Currie, S. Sen, Structural and Topological Control on Physical Properties of Arsenic Selenide Glasses, J. Phys. Chem. B. 118 (2014) 2284–2293.

[15] G. Yang, B. Bureau, T. Rouxel, Y. Gueguen, O. Gulbiten, C. Roiland, E. Soignard, J.L. Yarger, J. Troles, J.C. Sangleboeuf, P. Lucas, Correlation between structure and physical properties of chalcogenide glasses in the As_xSe_{1-x} system, Phys. Rev. B. 82 (2010) 195206.

[16] W. Zhu, I. Hung, Z. Gan, B. Aitken, S. Sen, Dynamical process related to viscous flow in a supercooled arsenic selenide glassforming liquid: Results from high-temperature ^{77}Se NMR Spectroscopy, J. Non. Cryst. Solids. 526 (2019) 119698.

[17] M. Kunugi, R. Ota, M. Suzuki, Viscosity of Glasses in the System As-Se, As-Se-S, As-Se-Te and As-Se-Tl, J. Soc. Mater. Sci. Jpn. 19 (1970) 145–150.

[18] S. V. Nemilov, G.T. Petrovskii, An Investigation of the Viscosity of Glasses of the Selenium-Arsenic Ststem, J. Appl. Chem. USSR. 36 (1963) 932–935.

[19] B. Yuan, B.G. Aitken, S. Sen, Rheology of supercooled P-Se glass-forming liquids: From networks to molecules and the emergence of power-law relaxation behavior, J. Chem. Phys. 156 (2022) 224502.

[20] M. Hart, J. Chen, A. Michaelides, A. Sella, M.S.P. Shaffer, C.G. Salzmann, One-Dimensional Arsenic Allotropes: Polymerization of Yellow Arsenic Inside Single-Wall Carbon Nanotubes, Angew. Chemie. 130 (2018) 11823–11827.

[21] B. Yuan, B. Aitken, S. Sen, Structural control on the rheological behavior of binary P-Se supercooled liquids, J. Non. Cryst. Solids. 559 (2021) 120669.

[22] J.C. Mauro, Y. Yue, A.J. Ellison, P.K. Gupta, D.C. Allan, Viscosity of glass-forming liquids, Proc. Natl. Acad. Sci. 106 (2009) 19780–19784.

[23] C. Zhang, L. Hu, Y. Yue, J.C. Mauro, Fragile-to-strong transition in metallic glass-forming liquids, J. Chem. Phys. 133 (2010) 14508.

[24] Y. Xia, B. Yuan, O. Gulbiten, B. Aitken, S. Sen, Kinetic and calorimetric fragility of chalcogenide glass-forming liquids: Role of shear vs enthalpy relaxation, J. Phys. Chem. B. 125 (2021) 2754–2760.

[25] G. Yang, O. Gulbiten, Y. Gueguen, B. Bureau, J.-C. Sangleboeuf, C. Roiland, E.A. King, P. Lucas, Fragile-strong behavior in the As_xSe_{1-x} glass forming system in relation to structural dimensionality, Phys. Rev. B - Condens. Matter Mater. Phys. 85 (2012) 144107.

[26] D.L. Sidebottom, Fragility of Network-Forming Glasses: A Universal Dependence on the Topological Connectivity, Phys. Rev. E. 92 (2015) 062804.

[27] S. Sen, H. Chen, Sources of Configurational Entropy versus Compositional Trends in

Fragility of Inorganic Glass-Forming Liquids, Phys. Status Solidi. 259 (2022) 2200002.

[28] B. Yuan, B. Aitken, I. Hung, Z. Gan, S. Sen, Compositional Evolution of the Structure and Connectivity in Binary P-Se Glasses: Results from 2D Multinuclear NMR and Raman Spectroscopy, J. Phys. Chem. B. 125 (2021) 13057–13067.

[29] A. Bytchkov, F. Fayon, D. Massiot, L. Hennet, D.L. Price, ^{31}P solid-state NMR studies of the short-range order in phosphorus-selenium glasses, Phys. Chem. Chem. Phys. 12 (2010) 1535–1542.

[30] D.G. Georgiev, M. Mitkova, P. Boolchand, G. Brunklaus, H. Eckert, M. Micoulaut, Molecular structure, glass transition temperature variation, agglomeration theory, and network connectivity of binary P-Se glasses, Phys. Rev. B. 64 (2001) 134204.

[31] R.T. Phillips, M.K. Ellis, Microstructure of P-Se glasses and low frequency Raman scattering, J. Non. Cryst. Solids. 164–166 (1993) 135–138.

[32] R.T. Phillips, D. Wolverson, M.S. Burdis, Y. Fang, Observation of discrete molecular structures in glassy P_xSe_{1-x} by Raman spectroscopy, Phys. Rev. Lett. 63 (1989) 2574–2577.

[33] V. Kovanda, M. Vlček, H. Jain, Structure of As-Se and As-P-Se glasses studied by Raman spectroscopy, J. Non. Cryst. Solids. 326–327 (2003) 88–92.

Figure Captions

Figure 1. Master curves of storage modulus G′ (squares) and loss modulus G″ (circles) of As_xSe_{100-x} supercooled liquids. Reference temperature for TTS corresponds to $\eta \sim 10^8$ Pa s in all cases and is listed alongside the composition in each plot. Solid straight-line segments mark the slopes in different frequency regions and green highlights indicate segments of constant slope for G′.

Figure 2. A representative simulation of the shear mechanical spectrum of $As_{55}Se_{45}$ supercooled liquid. Empty squares and circles represent the experimental G′ and G″ values, respectively. Long-dashed and short-dashed lines represent the fitted fast and slow relaxation processes, respectively. Solid lines are the total fit to the experimental data.

Figure 3. Temperature dependence of viscosity η of As_xSe_{100-x} liquids. Solid lines through the datapoints are fits to the MYEGA equation, where viscosity at $T = T_g$ is taken to be 10^{12} Pa.s and T_g values are taken from [15].

Figure 4. Composition dependence of fragility index *m* of As_xSe_{100-x} liquids determined in the present study (filled symbols) and reported in the literature (open symbols) [24].

Figure 5. Unpolarized Raman spectra of $P_{63}Se_{37}$ and $P_xAs_{4-x}Se_3$ glasses. Glass compositions are listed alongside the spectra.

Figure 6. Compositional evolution of the molecule:network ratio in $P_xAs_{4-x}Se_3$ glasses as obtained from Raman spectra in Fig. 5 (see text for details).

Figure 7. Temperature dependence of viscosity η of $P_xAs_{4-x}Se_3$ liquids. Lines through the symbols are guides to the eye.

Figure 8. Master curves of the frequency dependence of storage modulus G′ (squares) and loss modulus G″ (circles) of $P_xAs_{4-x}Se_3$ supercooled liquids with reference temperatures for TTS listed alongside the compositions in each panel. Solid straight-line segments mark the slopes in different frequency regions and green highlights indicate segments of constant slope for G′.

Fig. 1

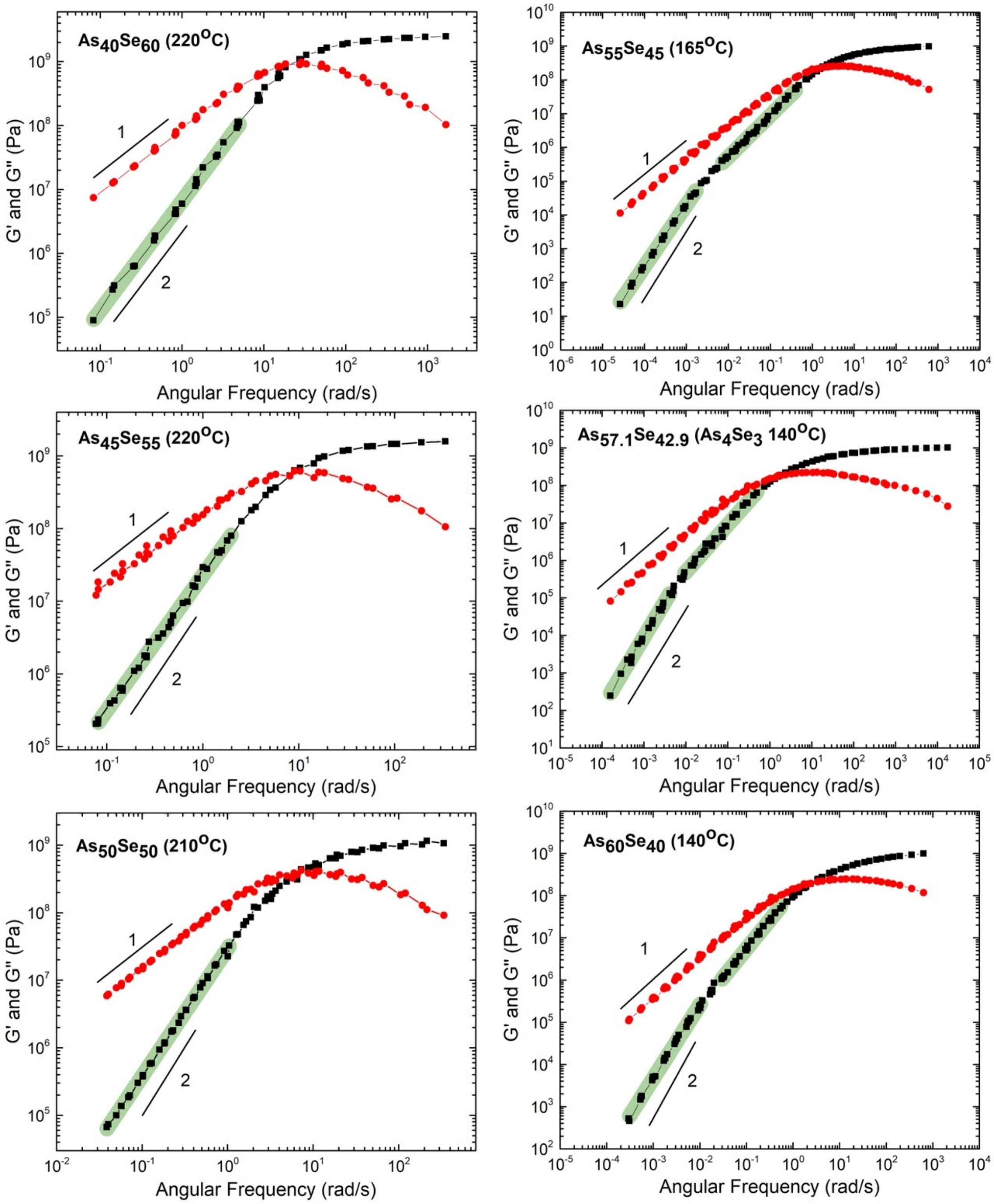
As40Se60 (220OC)
As55Se45 (165OC)
As45Se55 (220OC)
As57.1Se42.9 (As4Se3 140OC)
As50Se50 (210OC)
As60Se40 (140OC)
1
2
G' and G'' (Pa)
Angular Frequency (rad/s)

Fig. 2

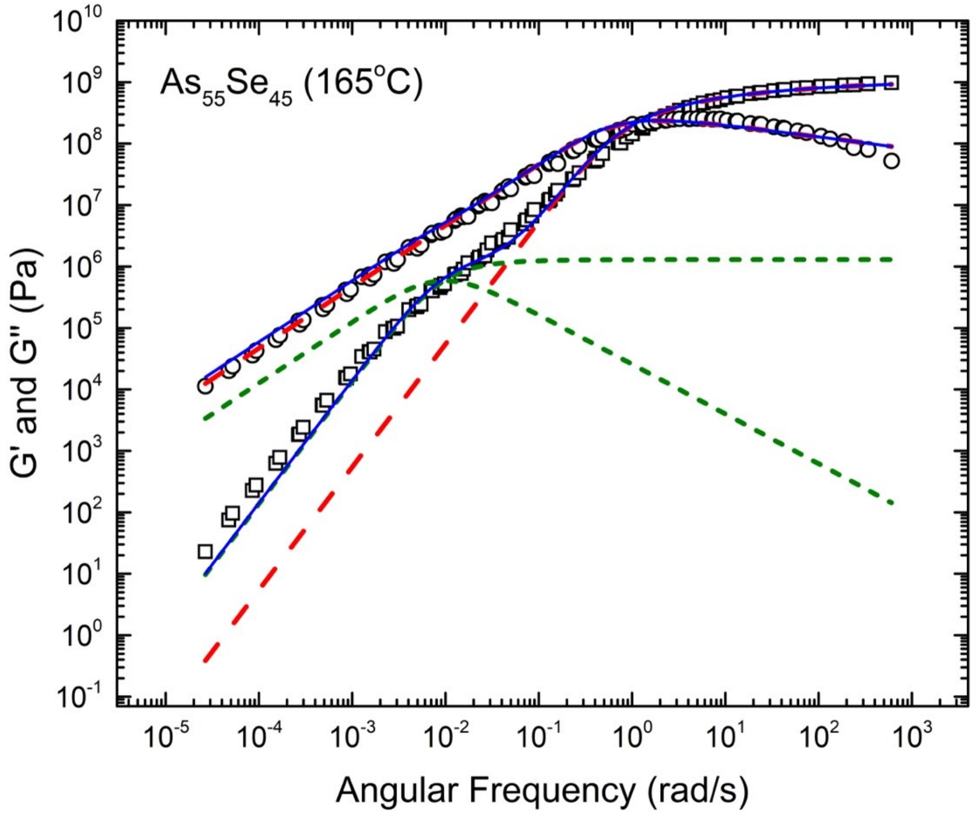
$As_{55}Se_{45}$ (165°C)
G' and G'' (Pa)
Angular Frequency (rad/s)
10^{10}
10^{9}
10^{8}
10^{7}
10^{6}
10^{5}
10^{4}
10^{3}
10^{2}
10^{1}
10^{0}
10^{-1}
10^{-5}
10^{-4}
10^{-3}
10^{-2}
10^{-1}
10^{0}
10^{1}
10^{2}
10^{3}

Fig. 3

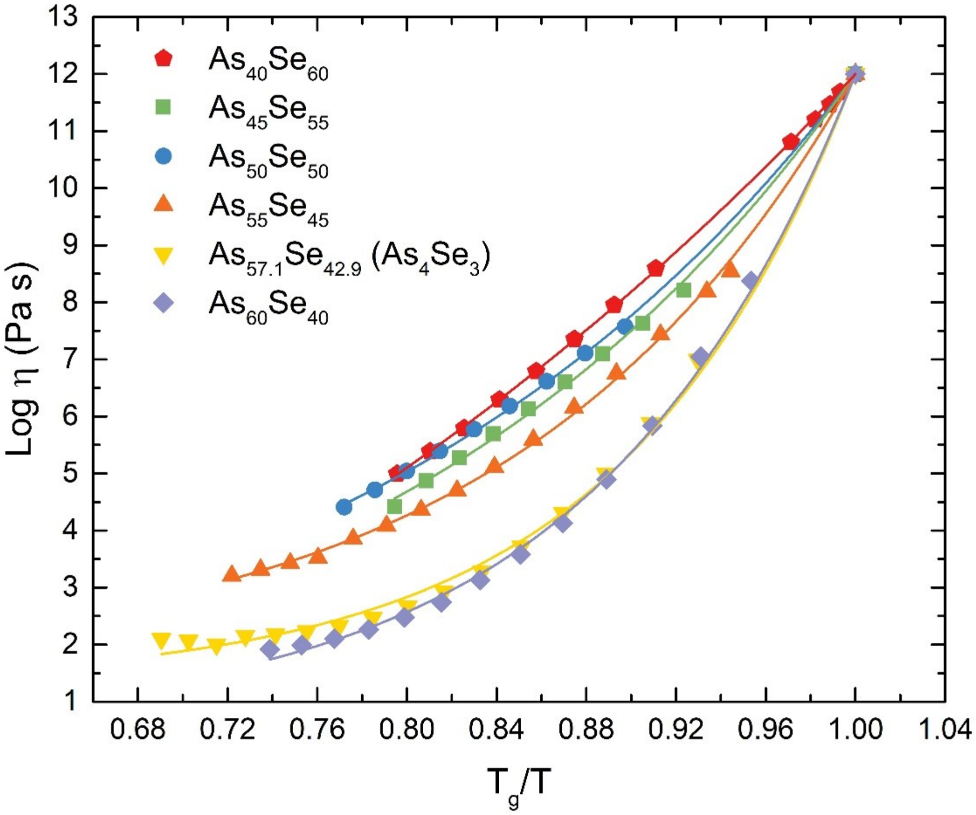
As40Se60
As45Se55
As50Se50
As55Se45
As57.1Se42.9 (As4Se3)
As60Se40
Log η (Pa s)
Tg/T
1
2
3
4
5
6
7
8
9
10
11
12
13
0.68
0.72
0.76
0.80
0.84
0.88
0.92
0.96
1.00
1.04

Fig. 4.

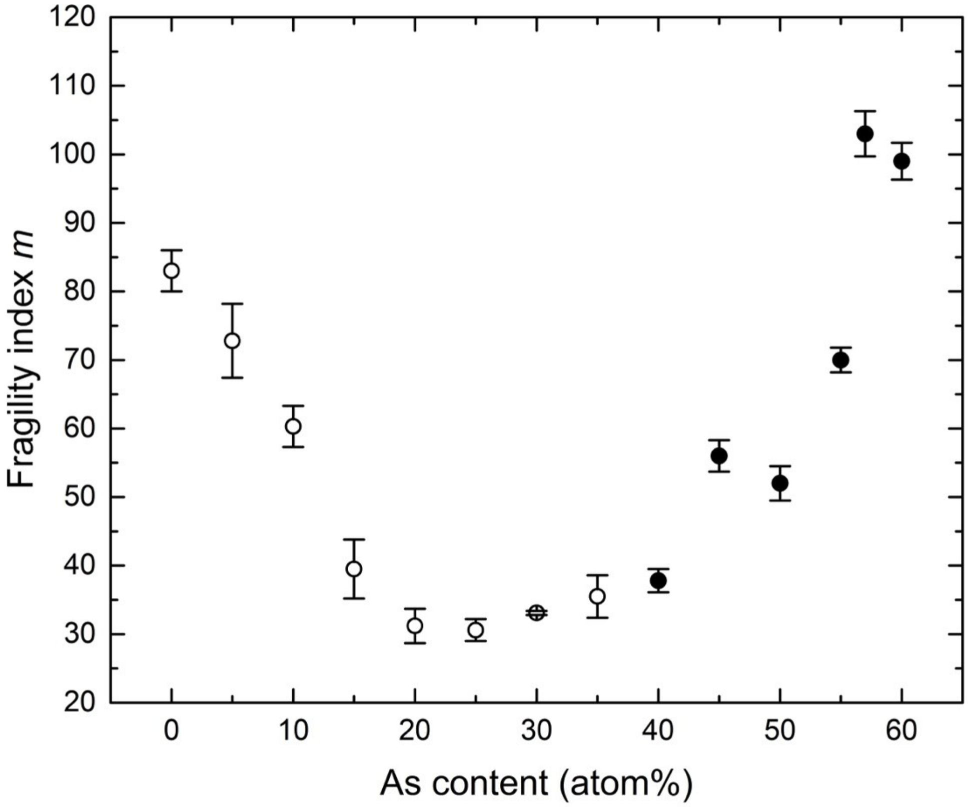

Fragility index *m*
120
110
100
90
80
70
60
50
40
30
20
0
10
20
30
40
50
60
As content (atom%)

Fig. 5

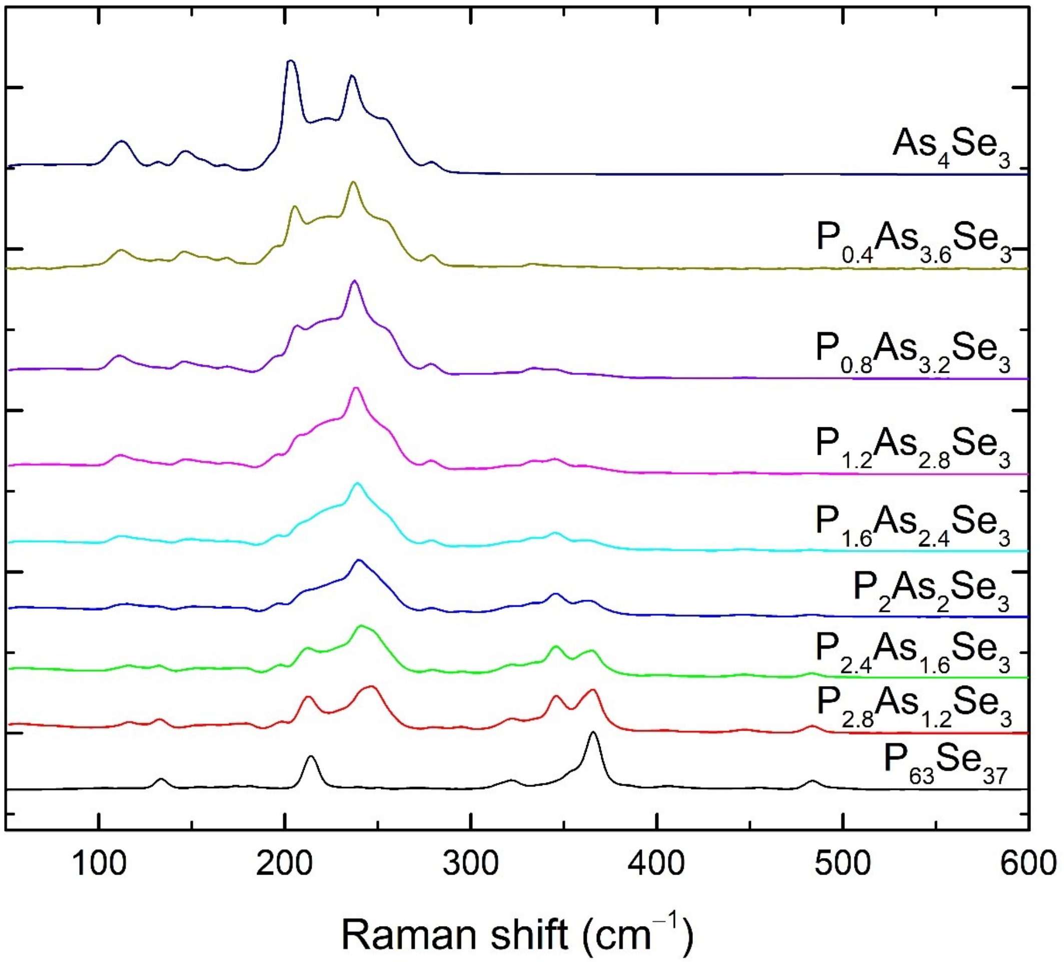

As_4Se_3
$P_{0.4}As_{3.6}Se_3$
$P_{0.8}As_{3.2}Se_3$
$P_{1.2}As_{2.8}Se_3$
$P_{1.6}As_{2.4}Se_3$
$P_2As_2Se_3$
$P_{2.4}As_{1.6}Se_3$
$P_{2.8}As_{1.2}Se_3$
$P_{63}Se_{37}$
100
200
300
400
500
600
Raman shift (cm^{-1})

Fig. 6

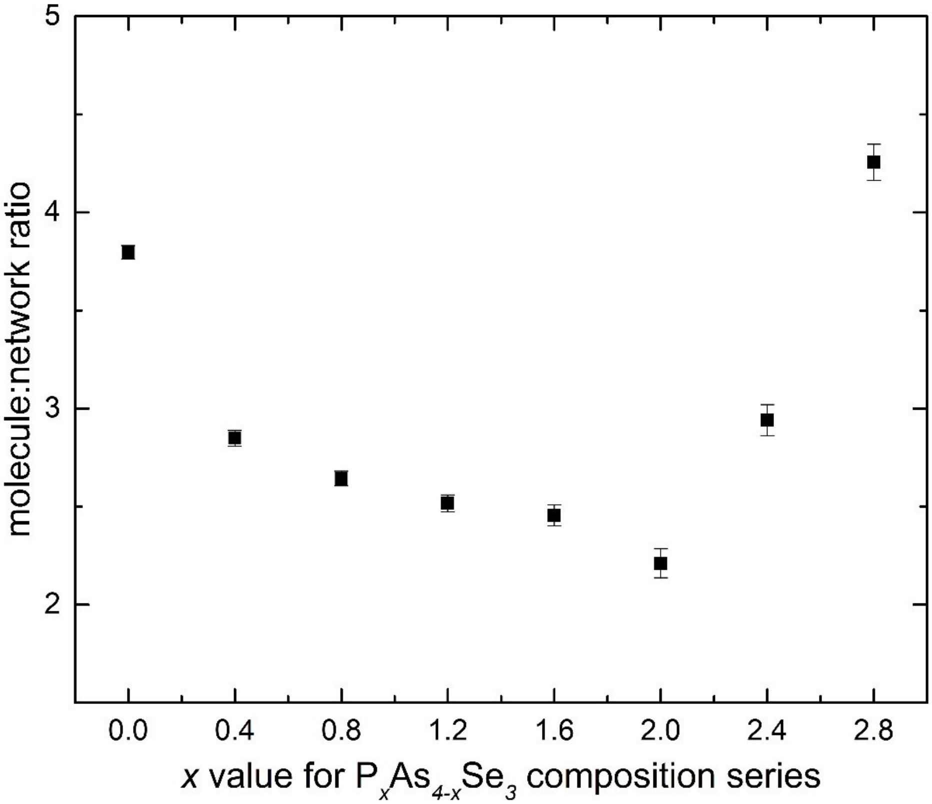

molecule:network ratio
5
4
3
2
0.0
0.4
0.8
1.2
1.6
2.0
2.4
2.8
x value for $P_xAs_{4-x}Se_3$ composition series

Fig. 7

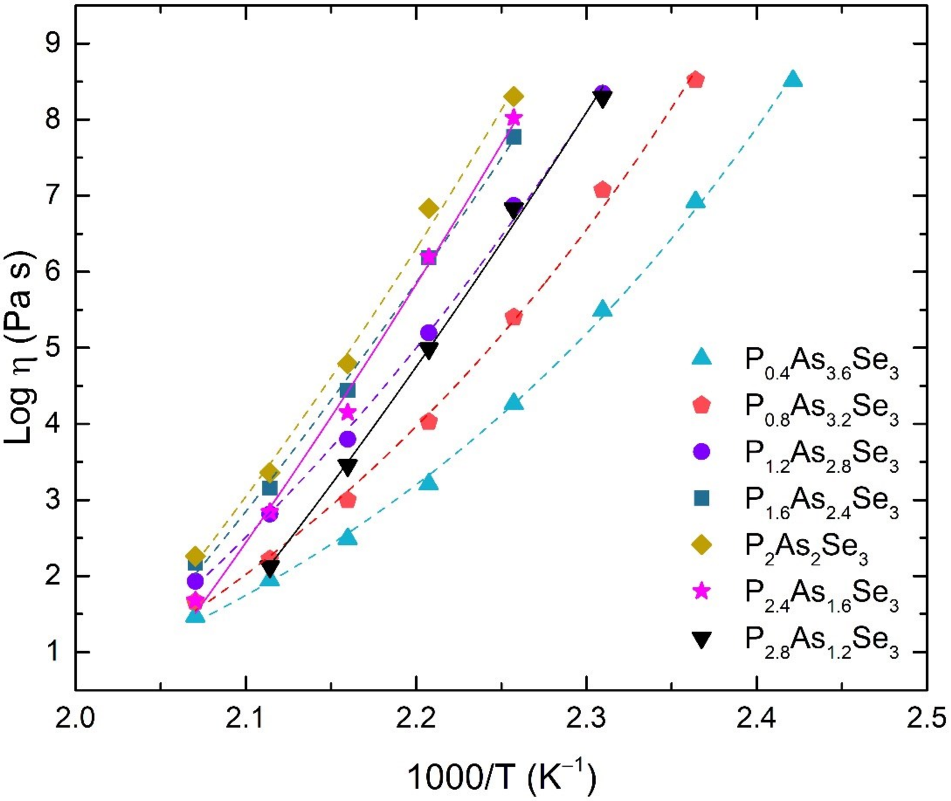

9
8
7
6
5
4
3
2
1
Log η (Pa s)
2.0
2.1
2.2
2.3
2.4
2.5
1000/T (K^{-1})
$P_{0.4}As_{3.6}Se_3$
$P_{0.8}As_{3.2}Se_3$
$P_{1.2}As_{2.8}Se_3$
$P_{1.6}As_{2.4}Se_3$
$P_2As_2Se_3$
$P_{2.4}As_{1.6}Se_3$
$P_{2.8}As_{1.2}Se_3$

Fig. 8

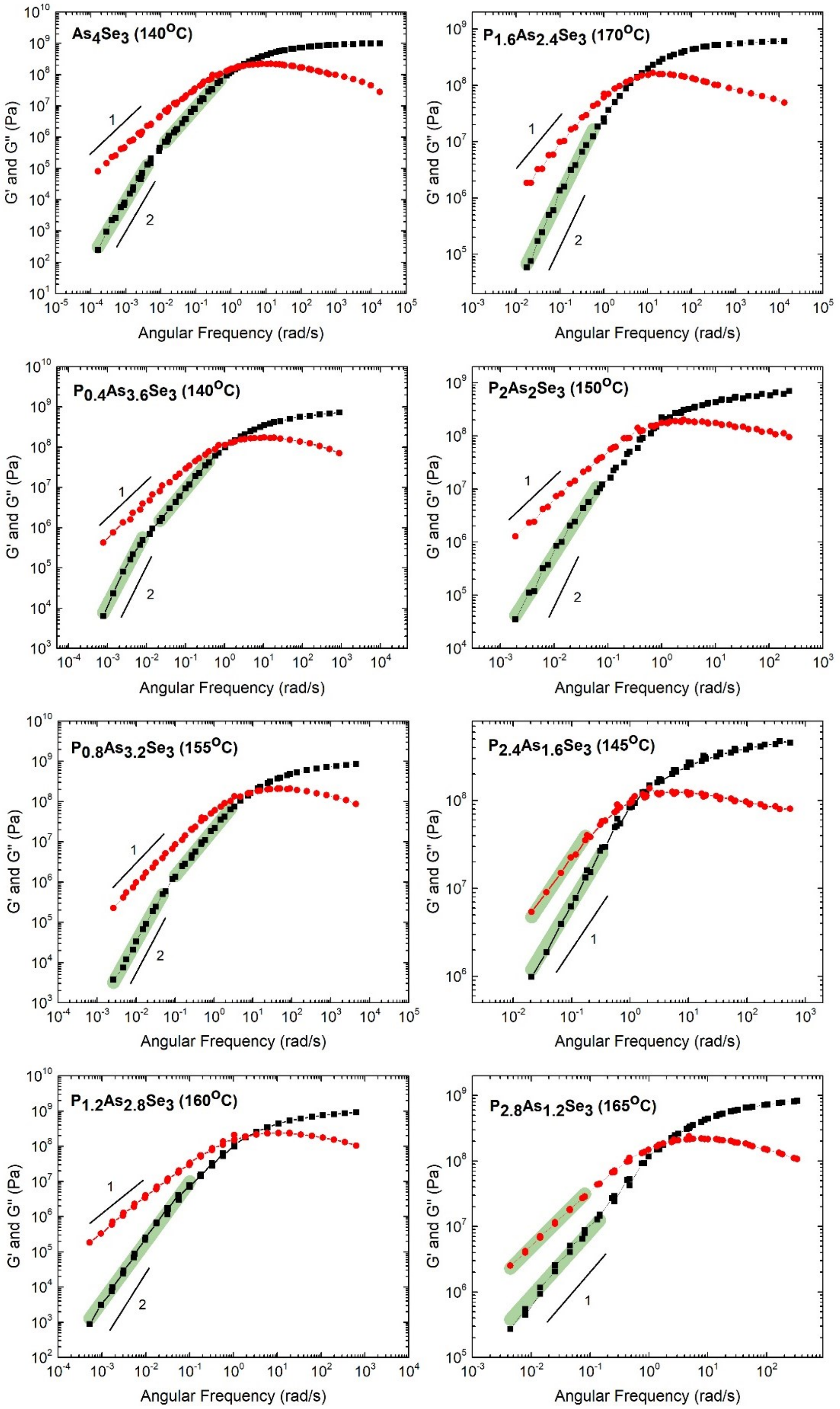

As$_4$Se$_3$ (140^{O}C)
P$_{1.6}$As$_{2.4}$Se$_3$ (170^{O}C)
P$_{0.4}$As$_{3.6}$Se$_3$ (140^{O}C)
P$_2$As$_2$Se$_3$ (150^{O}C)
P$_{0.8}$As$_{3.2}$Se$_3$ (155^{O}C)
P$_{2.4}$As$_{1.6}$Se$_3$ (145^{O}C)
P$_{1.2}$As$_{2.8}$Se$_3$ (160^{O}C)
P$_{2.8}$As$_{1.2}$Se$_3$ (165^{O}C)
G' and G'' (Pa)
Angular Frequency (rad/s)
1
2